

Revisiting NLO QCD corrections to total inclusive J/ψ and Υ photoproduction cross sections in lepton-proton collisions

Alice Colpani Serri^a, Yu Feng^b, Carlo Flore^a, Jean-Philippe Lansberg^a, Melih A. Ozcelik^{a,c}, Hua-Sheng Shao^d, Yelyzaveta Yedelkina^a

^aUniversité Paris-Saclay, CNRS, IJCLab, 91405 Orsay, France

^bDepartment of Physics, College of Basic Medical Sciences, Army Medical University, Chongqing 400038, China

^cInstitute for Theoretical Particle Physics, KIT, 76128 Karlsruhe, Germany

^dLaboratoire de Physique Théorique et Hautes Energies, UMR 7589, Sorbonne Université et CNRS, 4 place Jussieu, 75252 Paris Cedex 05, France

Abstract

We revisit the inclusive J/ψ and $\Upsilon(1S)$ photoproduction at lepton-hadron colliders, namely in the limit when the exchange photon is quasi real. Our computation includes the next-to-leading-order (NLO) α_s corrections to the leading-order contributions in v . Similarly to the case of NLO charmonium-hadroproduction processes, the resulting cross sections obtained in the $\overline{\text{MS}}$ factorisation scheme are sometimes found to be negative. We show that the scale-fixing criteria which we derived in a previous study of η_c production successfully solves this problem from the EicC all the way up to the FCC-eh energies. In turn, we investigate where both J/ψ and Υ photoproduction could be used to improve our knowledge of gluon densities at scales as low as a couple of GeV.

Keywords: J/ψ , Υ , ep reactions, photoproduction, HERA, EIC, EicC, AMBER-COMPASS++, LHeC, FCC-eh

1. Introduction

Inclusive production of quarkonia in hadron-hadron and lepton-hadron collisions is a potential rich source of information on the hadron structure. As such, it has been thoroughly studied both experimentally and theoretically (see [1–6] for reviews). Yet, the mechanisms underlying their inclusive production are still not an object of consensus within the community. This in turn does not comfort one to employ cross-section measurements to extract information on the gluon structure of the proton.

In a recent study [7], we have however shown that the large- P_T inclusive J/ψ photoproduction data can be accounted for by the Colour-Singlet Model (CSM) [8–10], *i.e.* the leading- v contribution of Non-Relativistic QCD (NRQCD) [11]. In the photoproduction limit, a quasi on-shell photon hits and breaks a proton to produce the J/ψ usually along with at least a recoiling hard parton. This limit has been studied in detail at HERA [12–18] to decipher the quarkonium-production mechanisms and then to probe the gluon content of the proton (see *e.g.* [19]). As expected, photoproduction indeed seems to be more easily understandable than hadroproduction [6]¹. It is also believed that quarkonium production in lepton-proton collisions

could be used to measure Transverse Momentum Dependent gluon distributions (see *e.g.* [20–23]).

Owing to the presence of an electromagnetic coupling, photoproduction cross sections are smaller than hadroproduction ones which calls for large luminosities to obtain large enough quarkonium data sets. As such, the P_T reach of J/ψ HERA data is limited to barely 10 GeV, there is quasi no data on ψ' and none on the Υ .

In the present analysis, we focus on the P_T -integrated yields which was surprisingly seldom studied at HERA. Indeed most of the inclusive data set have been selected with the minimal P_T of 1 GeV. This cut however introduces a strong sensitivity on the P_T spectrum of the cross section in a region where it is not necessarily well controlled. By itself, such a yield is not directly connected to the total number of J/ψ produced for which we believe the theory predictions to be more robust. One reason for such a cut is probably the difficulty to obtain numerically stable NLO results when they appeared [24, 25]². In fact, as we will discuss, these were probably due to the appearance of large negative NLO contributions which we will address here along the same lines as our recent study on η_c production [27].

Moreover, such P_T -integrated cross sections will be easily measurable at high energies with a very good accuracy at the planned US Electron-Ion Collider (EIC) [28],

Email addresses: carlo.flore@ijclab.in2p3.fr (Carlo Flore), jean-philippe.lansberg@in2p3.fr (Jean-Philippe Lansberg), melih.ozcelik@kit.edu (Melih A. Ozcelik), huasheng.shao@lpthe.jussieu.fr (Hua-Sheng Shao), yelyzaveta.yedelkina@universite-paris-saclay.fr (Yelyzaveta Yedelkina)

¹At high energies, the hadronic content of the photon can be “resolved” during the collisions. Resolved-photon – proton collisions are very similar

to those for hadroproduction and are interesting of their own. We will however disregard them in the present discussion and they can be avoided by a simple kinematical cut on low elasticity values, z . Along the same lines, exclusive or diffractive contributions can be also avoided by cutting z close to unity.

²In particular, we note the reference [48] of [26].

but also at future facilities such as the LHeC [29] or FCC-eh [30], thus in a region where the gluon PDFs are not well constrained. Measurements at lower energies at AMBER-COMPASS++ [31], the EicC [32] would then rather probe the valence region, which could happen to be equally interesting.

In our study, like in the previous one [7], we will focus on the aforementioned CSM [9], corresponding to the leading- v contribution in NRQCD whose NLO QCD corrections are in principle known since the mid nineties [24, 25]. As we revisited in [7], the impact of QCD corrections to J/ψ inclusive photoproduction steadily grows when P_T increases. This can be traced back to the more favourable P_T scaling of specific real-emission contributions. The same has been observed in several quarkonium-hadronproduction processes, including those of spin-triplet vector quarkonia [33–39] (denoted \mathcal{Q}). On the contrary, one expects, at low P_T , a more subtle interplay between the contribution of these real emissions near the collinear region and the loop corrections. This has for a long time been understudied. We thus aim at discussing it here in detail.

The structure of our Letter is as follows. Section 2 outlines our methodology to compute vector-quarkonium inclusive photoproduction cross sections at NLO accuracy including a discussion of the reason for negative NLO cross sections and our proposed solution. Section 3 gathers our prediction for future measurements the lepton-hadron colliders along with a discussion of the corresponding theoretical uncertainties. Section 4 gathers our conclusions.

2. J/ψ and Υ photoproduction up to one-loop accuracy

2.1. Elements of kinematics

We will consider the reaction $\gamma(P_\gamma)+p(P_p) \rightarrow \mathcal{Q}(P_Q)+X$ where the photon $\gamma(P_\gamma)$ is emitted by an electron $e(P_e)$. Let us then define $s_{ep} = (P_e + P_p)^2 \approx 4E_e E_p + m_p^2$ (E_e is the electron (proton) beam energy, m_p is the proton mass) and $s_{\gamma p} = W_{\gamma p}^2 = (P_\gamma + P_p)^2$. We can then introduce x_γ as $P_\gamma = x_\gamma P_e$ such as $s_{\gamma p} = x_\gamma s_{ep}$. As announced, in the present study, $P_\gamma^2 \simeq 0$.

Diffractive contributions are suppressed for increasing P_T and away from the exclusive limit, *i.e.* when the quarkonium carries nearly all the photon momentum. A cut on P_{QT} is usually sufficient to get rid of them, which we do not wish to apply here. One can however cut on a variable called elasticity, defined as $z = \frac{P_Q \cdot P_p}{P_\gamma \cdot P_p}$. z indeed corresponds to the fraction of the photon energy taken by the quarkonium in the proton rest frame, with the proton momentum defining the z axis. It can be rewritten as $z = \frac{2E_p m_T}{W_{\gamma p}^2 e^y}$ in terms of the quarkonium rapidity y (with y and E_p being defined in the same frame) and the quarkonium transverse mass, $m_T = \sqrt{M_Q^2 + P_{QT}^2}$ with M_Q being the quarkonium mass. Such diffractive contributions are known to lie at $z \rightarrow 1$ [12]. At low z , resolved-photon contributions can appear as important where only a small fraction of the photon energy is involved in the quarkonium production. At

HERA, they had a limited impact [1, 12]. At lower energies, like at the EIC, their impact should be further reduced. On the contrary, at the LHeC or FCC-eh, their impact might be sizable even at moderate z . Nonetheless, their modelling requires a good control of the contributions from gg and gq channels. However, our understanding of the very same channels in inclusive quarkonium hadronproduction, especially at low P_T [6], is clearly limited. When comes the time for the building of these future lepton-hadron colliders, it will be needed to re-evaluate the impact of the resolved-photon contributions at low z and high energies. For the time being, we simply note that imposing a lower bound on z would not alter our conclusions at all, precisely because it does not correspond to the low- x region in the proton.

2.2. The Colour-Singlet Model

As aforementioned, there is no agreement on which mechanism is dominant in quarkonium production. The most popular approaches are: the Colour-Singlet Model (CSM) [8–10], the Colour-Evaporation Model (CEM) [40, 41] and the Non-Relativistic QCD (NRQCD) [11], whose leading- v contribution is the CSM for S -wave quarkonia. These mechanisms mainly differ in the way they describe hadronisation.

The factorisation approach of the CSM is based on considering only the leading Fock states of NRQCD. In the CSM, there is no gluon emission during the hadronisation process, and, consequently, the quantum state $Q\bar{Q}$ does not evolve during the binding. Thus, spin and colour remain unchanged.

With a projection operator, which associates a γ_5 matrix to pseudo-scalars (η_c, η_b) and γ_μ to vectors ($J/\psi, \Upsilon(1S)$), we can use the Feynman graphs to compute the perturbative amplitude to produce the $Q\bar{Q}$ pair. As we impose the $Q\bar{Q}$ relative momentum $p = (p_Q - p_{\bar{Q}})/2$ to vanish, the spin projector on a vector state can be written as:

$$N(\lambda|s_i, s_j) = \frac{1}{2\sqrt{2}m_Q} \bar{v}\left(\frac{\mathbf{P}_Q}{2}, s_j\right) \epsilon_\mu^\lambda \gamma^\mu u\left(\frac{\mathbf{P}_Q}{2}, s_i\right), \quad (1)$$

where s_1 and s_2 are the heavy-quark spins, m_Q is the heavy-quark mass, ϵ_μ^λ is the polarisation vector of a quarkonium with a polarisation λ , and the total quarkonium momentum is $P_Q = p_Q + p_{\bar{Q}}$.

The matrix element \mathcal{M} to produce a vector state $Q + \{k\}$, where $\{k\}$ is a set of final state particles, from the scattering of the partons ab in CSM is:

$$\mathcal{M}(ab \rightarrow Q + \{k\}) = \sum_{s_1, s_2, i, i'} \frac{N(\lambda|s_1, s_2)}{\sqrt{m_Q}} \frac{\delta^{ii'}}{\sqrt{N_c}} \frac{R(0)}{\sqrt{4\pi}} \times \mathcal{M}(ab \rightarrow Q_i^{s_1} \bar{Q}_{i'}^{s_2}(\mathbf{p} = \mathbf{0}) + \{k\}), \quad (2)$$

where $\delta^{ii'}/\sqrt{N_c}$ is the projector onto a CS state and $\mathcal{M}(ab \rightarrow Q\bar{Q} + \{k\})$ is the amplitude to create the corresponding heavy-quark pair. When one then sums over the heavy-quark spins, one obtains usual traces which can be

evaluated without any specific troubles. In fact, such a computation can be automated at tree level as done by HELAC-ONIA [42, 43]. In the present case of inclusive photoproduction of a vector Q , there is a single partonic process at Born order, $\alpha\alpha_s^2$, namely $\gamma g \rightarrow Qg$ (see Fig. 1a). In principle, one could also consider $\gamma Q \rightarrow QQ$ at the same order, but we have shown it to be small at low P_T [7].

The value of $R(0)$, the Q radial wave function at the origin in the configuration space, can be in principle extracted from the leptonic decay width computed likewise in the CSM. The latter is known up to NLO [44] since the mid 70's, up to NNLO since the late 90's [45, 46] and up to N³LO since 2014 [47]. However, as discussed in Appendix A, the short-distance amplitude receives very large QCD radiative corrections which translate into significant renormalisation and NRQCD-factorisation scale uncertainties. These essentially preclude drawing any quantitative constraints on $R(0)$ from the leptonic decays width.

In principle, we should thus associate to it a specific theoretical uncertainty which is however supposed to only affect the normalisation of the cross sections. In what follows, we will employ a similar value as Krämer [25], 1.25 GeV³ for the J/ψ and 7.5 GeV³ for the $\Upsilon(1S)$. As for the masses, we will use $m_c = 1.5$ GeV and $m_b = 4.75$ GeV. Let us recall that within NRQCD $M_Q = 2m_Q$.

Fig. 1a displays one of the six Feynman diagrams for inelastic Q photoproduction at LO ($\alpha\alpha_s^2$). At this order, only photon-gluon fusion contributes. After averaging over colour/helicities of the initial gluon/photon the amplitude squared computed according to Eq. (2), one obtains the averaged amplitude squared (see e.g. [9, 25])³:

$$\begin{aligned} \overline{|\mathcal{M}_{\gamma g}^{(0)}|^2} &= \frac{\alpha\alpha_s^2(\mu_R)e_Q^2 |R(0)|^2}{M_Q^2 4\pi M_Q^3} 384\pi^3 M_Q^6 \times \\ &\times \frac{\hat{s}^2(\hat{s} - M_Q^2)^2 + \hat{t}^2(\hat{t} - M_Q^2)^2 + \hat{u}^2(\hat{u} - M_Q^2)^2}{(\hat{s} - M_Q^2)^2(\hat{t} - M_Q^2)^2(\hat{u} - M_Q^2)^2}, \end{aligned} \quad (3)$$

with the partonic Mandelstam variables in the photon-proton center-of-mass (c.m.) frame:

$$\begin{aligned} \hat{s} &= (P_\gamma + xP_p)^2 = xs_{\gamma p}, \\ \hat{t} &= (P_Q - P_\gamma)^2 = M_Q^2 - \sqrt{s_{\gamma p}}m_T e^y, \\ \hat{u} &= (P_Q - xP_p)^2 = M_Q^2 - x\sqrt{s_{\gamma p}}m_T e^{-y}, \end{aligned} \quad (4)$$

where x is the longitudinal momentum fraction of the proton carried by the parton.

The partonic cross section can then be obtained from:

$$\frac{d\hat{\sigma}_{\gamma g}^{(0)}}{d\hat{t}} = \frac{1}{16\pi\hat{s}^2} \overline{|\mathcal{M}_{\gamma g}^{(0)}|^2}. \quad (5)$$

Doing so, the hadronic cross section is readily obtained by folding $d\hat{\sigma}_{\gamma g}^{(0)}$ with the corresponding PDFs and, if relevant, summing over the parton species. Generically, one

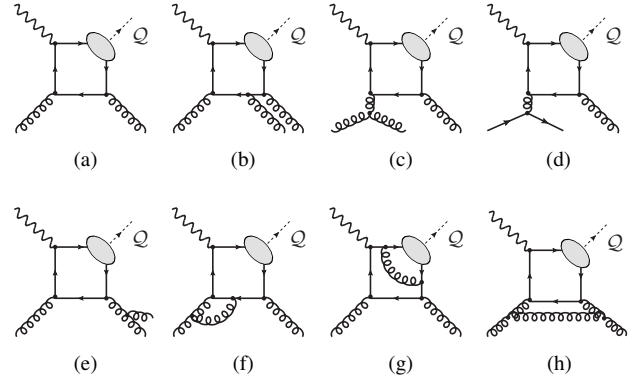


Figure 1: Representative Feynman diagrams for inelastic Q photoproduction contributing via CS channels at orders $\alpha\alpha_s^2$ (a), $\alpha\alpha_s^3$ (b,c,d,e,f,g,h). The quark and anti-quark attached to the ellipsis are taken as on-shell and their relative velocity v is set to zero.

indeed has:

$$d\sigma_{\gamma p}(s_{\gamma p}, m_Q^2) = \sum_{i=g,q,\bar{q}} \int dx f_i(x, \mu_F) d\hat{\sigma}_{\gamma i}. \quad (6)$$

where μ_F is the factorisation scale, $f_i(x, \mu_F)$ is the PDF that gives the probability that a parton i carries a momentum fraction x of the parent proton. At LO, $d\hat{\sigma}_{\gamma i}^{(0)}$ identifies to $d\hat{\sigma}_{\gamma g}^{(0)}$.

2.3. The NLO corrections and their divergences

At order $\alpha\alpha_s^3$, two categories of new contributions arise. Those from the real emissions represented by Fig. 1b, 1c, 1d, 1e and from virtual emissions (or loops) represented by Fig. 1f, 1g, 1h. Specific topologies of the former category benefit from P_T/M_Q enhancement factors which make them leading at large P_T . This for instance justifies to employ the NLO* approximation [7]. When P_T is integrated over, a priori all these contributions should be accounted for. Such a computation was first carried out by Krämer [24] in the mid 1990's. We will briefly outline now what it amounts to.

As usual, one critical feature of such NLO computations in collinear factorisation [48] is the appearance of various types of singularities. In order to tackle these, one usually resorts to dimensional regularisation whereby one shifts the dimensions from $d = 4$ to $d = 4 - 2\epsilon$, and the singularities of the various divergent contributions appear as poles in ϵ . This helps us to achieve their cancellations when all the contributions are summed (after factorisation, renormalisation and the phase-space integration).

Both virtual and real emissions are sources of divergences. The latter only exhibit low-energy, infrared (IR) ones. These are of two types: soft and collinear. The soft ones arise from the emission of a massless gauge boson with vanishing energy. The real-emission contributions indeed involve an additional particle and the divergences appear after the phase-space integration. Such soft singularities should match those of the virtual-emission contributions and cancel. From the latter, also called loop corrections, one can indeed distinguish (high-energy) ultraviolet (UV) and IR singularities. The former can be removed

³LO contributions will be labelled with an exponent 0 in parenthesis and the NLO with 1.

via the procedure of renormalisation⁴. The latter cancel the aforementioned soft singularities from the real emissions. See [50] for a recent textbook on such matter.

On the other hand, collinear divergences arise when one cannot distinguish two massless particles, with an angle between them close to zero. Those from final-state emissions disappear when the phase space is integrated over according to the KLN theorem [51, 52]. On the contrary, initial-state ones remain because the initial states are fixed by the kinematics of collinear factorisation and, consequently, are not fully integrated over. These singularities are absorbed inside the $\overline{\text{MS}}$ -renormalised PDFs via the process-independent Altarelli-Parisi Counter Terms (AP-CT). This kind of divergences, on which we will elaborate further, is thus specific to collinear factorisation. These AP-CT introduce a μ_F dependence in the partonic cross section, which would, in an all-order computation, cancel that introduced by the PDF scale evolution governed by the DGLAP equation. As for the renormalisation scale, μ_R , it appears via the running of α_s and the renormalisation of the UV divergences, as usual.

Gluon radiations from a massive quark (Fig. 1b) do not generate any collinear divergences, only soft ones. For the present process, such a soft divergence does not appear because the contributions from the heavy quark and antiquark cancel for $p = 0$ and colour-singlet S -wave $Q\bar{Q}$ states. For the diagrams of Fig. 1c and Fig. 1d and similar, the emission of a soft or collinear gluon/quark attached to the initial gluon/(light) quark generate divergences. The diagrams depicted in Fig. 1e also exhibit both soft and collinear singularities which should disappear after integration according to the KLN theorem.

2.4. The cross section in terms of scaling functions

For our analysis, we have found useful to employ the NLO cross-section decomposition in terms of scaling functions derived by Krämer [25]. Using FDC [36, 53], we have reproduced his results (scaling functions as well as hadronic cross sections) and, with the appropriate parameter choices and kinematical cuts, those of [54].

Indeed, the advantage of considering P_T - and z -integrated cross sections is that the hadronic photoproduction cross sections can be recast in terms of a simple convolution of the PDF and scaling functions of a single scaling variable⁵. This allows one to outline the structure of the result to better understand some specific behaviour (like the scale dependencies discussed in the previous section, hence the importance of negative contributions to the cross section) of the NLO yield. This formulation is also useful because it allows one to vary economically parameters like the c.m. energy, the heavy-quark mass, the renormalisation and factorisation scales.

⁴For inclusive quarkonium production, one usually resorts to the on-shell (OS) renormalisation scheme for the gluon/quark wave functions and for the heavy-quark mass, and the $\overline{\text{MS}}$ -scheme renormalisation for the coupling, see e.g. [25, 49].

⁵In what follows, we will show them as a function of \hat{s} and m_Q but they can equally be written as a function of $\eta = \hat{s}/4m_Q^2 - 1$.

Along the lines of Krämer [25], we express the partonic cross section as⁶:

$$\begin{aligned} \hat{\sigma}_{\gamma i}(\hat{s}, m_Q^2, \mu_R, \mu_F) &= \frac{\alpha\alpha_s^2(\mu_R)e_Q^2}{m_Q^2} \frac{|R(0)|^2}{4\pi m_Q^3} \times \\ &\times \left[c_{\gamma i}^{(0)}(\hat{s}, m_Q^2) + 4\pi\alpha_s(\mu_R) \left\{ c_{\gamma i}^{(1)}(\hat{s}, m_Q^2) + \bar{c}_{\gamma i}^{(1)}(\hat{s}, m_Q^2) \ln \frac{M_Q^2}{\mu_F^2} \right. \right. \\ &\left. \left. + \frac{\beta_0(n_{lf})}{8\pi^2} c_{\gamma i}^{(0)}(\hat{s}, m_Q^2) \ln \frac{\mu_R^2}{\mu_F^2} \right\} \right], \end{aligned} \quad (7)$$

where $i = g, q, \bar{q}$, $\beta_0(n_{lf}) = (11N_c - 2n_{lf})/3$, with n_{lf} the number of active (light) flavours. The scaling functions are shown on Fig. 2. $c_{\gamma g}^{(0)}$ arises from the $\alpha\alpha_s^2$ (LO) γg contributions, while $c_{\gamma g}^{(1)}$ and $\bar{c}_{\gamma g}^{(1)}$ from the $\alpha\alpha_s^3$ (NLO) γg contributions and $c_{\gamma q}^{(1)}$ and $\bar{c}_{\gamma q}^{(1)}$ from the $\alpha\alpha_s^3$ (NLO) γq contributions. $c_{\gamma g}^{(1)}$ encapsulates contributions⁷ from both real- and virtual emissions. If it had contained only virtual contributions, it would scale like $c_{\gamma g}^{(0)}$ and eventually vanish at large \hat{s} . This implies that the asymptotic value of $c_{\gamma g}^{(1)}$ entirely comes from the real emissions. $\bar{c}_{\gamma g}^{(1)}$ only includes real emissions and comes along with an explicit μ_F dependence from the AP-CT. The last term, whose form is generic, comes from the renormalisation procedure. The hadronic cross section is then obtained according to Eq. (6).

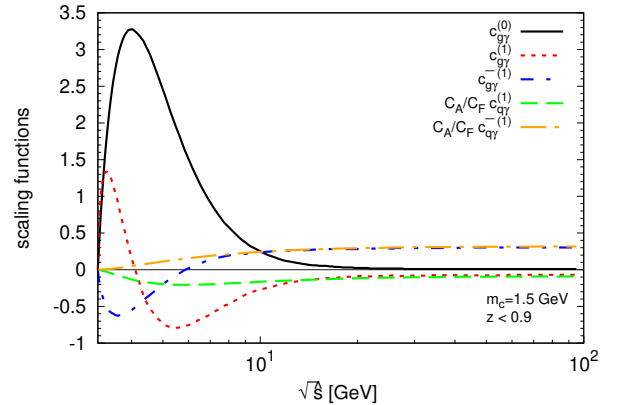


Figure 2: Scaling functions as function of $\sqrt{\hat{s}}$, where $C_A = 3$, $C_F = 4/3$.

Already at this stage, we can note then that, at large \hat{s} , the NLO cross section will be proportional to $\ln(M_Q^2/\mu_F^2)$ and a process-dependent coefficient, $\bar{c}_{\gamma i}^{(1)}(\hat{s} \rightarrow \infty, m_Q^2)$, which only comes on the real-emission contributions, like for η_Q hadroproduction [27].

Fig. 3 shows the $\sqrt{s_{\gamma p}}$ -dependence of $\sigma_{\gamma p}$ for J/ψ photoproduction integrated over $z < 0.9$ and P_T , for different choices of μ_R and μ_F among $M_{J/\psi} \times (0.5, 1, 2)$, using the

⁶The scaling functions were derived in the $\overline{\text{MS}}$ factorisation scheme. Here $\bar{c}^{(1)}$ and $c^{(1)}$ correspond to $-\bar{c}^{(1)}$ and $c^{(1)} + \ln 4\bar{c}^{(1)}$ defined by Krämer [25].

⁷To be exact, the corresponding term should in principle exhibit a n_f dependence from $\gamma g \rightarrow Qq\bar{q}$. The difference between the case J/ψ and $\Upsilon(1S)$ would be from $\gamma g \rightarrow Qc\bar{c}$ with $m_c = 0$ which can safely be neglected.

CT18NLO PDF set [55] and with a 20% feed-down contribution from ψ' decay (as in [7]). We expect the b feed down on the P_T -integrated yields to be on the order of 5% and we do not include it as it can be experimentally removed.

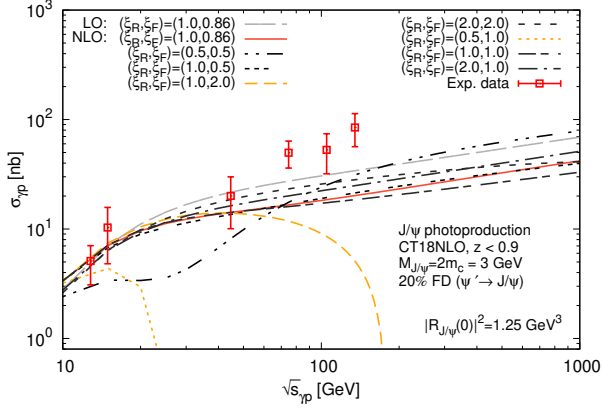


Figure 3: LO and NLO $\sigma_{\gamma p}$ as a function of $\sqrt{s_{\gamma p}}$ for J/ψ photoproduction for different scale choices (with the notation $\xi_{R,F} \equiv \mu_{R,F}/M_{J/\psi}$) compared with experimental data: H1 [25], FTPS [56], NA14 [57].

The long dashed grey curve is the LO cross section for $\mu_R = M_Q$ and $\mu_F = 0.86 M_Q$. We have checked that it remains positive for any μ_R and μ_F scale choice which is expected provided that the PDFs are positive. It happens to reasonably account for the available experimental values if one notes that the theoretical uncertainties from the scales, the mass and $R(0)$ (not shown) are significant. All other curves represent the NLO cross section for different scale choices. In two cases, the NLO cross section becomes negative as $s_{\gamma p}$ increases. As for $\Upsilon(1S)$, the cross section remains positive in the considered energy range for any realistic scale choice, like for η_b hadroproduction up to 100 TeV [27]. Let us now discuss the origin of such an unphysical behaviour for J/ψ photoproduction and propose a solution to it.

2.5. A new scale prescription to cure the unphysical behaviour of the NLO quarkonium photo-production

From the above discussion, there can only be two sources of negative partonic cross sections: the loop amplitude via interference with the Born amplitude and the real emissions via the subtraction of the IR poles from the initial-emission collinear singularities. As we will argue now, the latter subtraction is the source of the negative cross section which we have just uncovered. As it was mentioned before, such divergences are removed by subtraction into the PDFs via AP-CT and the high-energy limit of the resulting partonic cross section takes the form:

$$\lim_{\hat{s} \rightarrow \infty} \hat{\sigma}_{\gamma i}^{\text{NLO}} \propto \left(\log \frac{M_Q^2}{\mu_F^2} + A_{\gamma i} \right), A_{\gamma g} = A_{\gamma q}, \quad (8)$$

where $A_{\gamma i} = c_{\gamma i}^{(1)}(\hat{s} \rightarrow \infty, m_Q^2) / \bar{c}_{\gamma i}^{(1)}(\hat{s} \rightarrow \infty, m_Q^2)$ are the coefficients of the finite term of NLO cross section in the high-energy limit. As can be seen from Fig. 2, $A_{\gamma i}$ is negative

for $z < 0.9$, i.e. -0.29 . It is also clear from Fig. 2 that $A_{\gamma g} = A_{\gamma q}$.

Unless μ_F is sufficiently smaller than M_Q in order to compensate $A_{\gamma i}$, $\lim_{\hat{s} \rightarrow \infty} \hat{\sigma}_{\gamma i}^{\text{NLO}}$ is negative, like for η_Q [27] and it is another clear case of oversubtraction by the AP-CT. Indeed, in this limit, the virtual contributions are suppressed; only the real emissions contribute via their square. As such, they can only yield positive partonic cross sections before the subtraction of the initial-state collinear divergences. The sole source of negative contribution is therefore the AP-CT.

In principle, the negative term from the AP-CT should be compensated by the evolution of the PDFs according to the DGLAP equation. Yet, for the μ_F values on the order of the natural scale of these processes, the PDFs are not evolved much and can sometimes be so flat for some PDF parametrisations that the large \hat{s} region still significantly contributes. This results in negative values of the hadronic cross section. Indeed, $A_{\gamma g}$ and $A_{\gamma q}$ are process-dependent, while the DGLAP equations are process-independent, which necessarily makes the compensation imperfect. A solution to this problem is [27] to force the partonic cross section to vanish in this limit, whose contribution should in principle be damped down by the PDFs.

According to this prescription, one needs to choose μ_F such that $\lim_{\hat{s} \rightarrow \infty} \hat{\sigma}_{\gamma i}^{\text{NLO}} = 0$. It happens to be possible since $A_{\gamma g} = A_{\gamma q}$. This amounts to consider that all the QCD corrections are in the PDFs [27]. From Eq. (8), we have:

$$\mu_F = \hat{\mu}_F = M_Q e^{A_{\gamma i}/2} = M_Q \exp \left(\frac{c_{\gamma i}^{(1)}(\hat{s} \rightarrow \infty, m_Q^2)}{2\bar{c}_{\gamma i}^{(1)}(\hat{s} \rightarrow \infty, m_Q^2)} \right). \quad (9)$$

Using the scaling function of Fig. 2 when one fully integrates over P_T and over $z < 0.9$, one gets $\hat{\mu}_F = 0.86 M_Q$. From now on, all our results will be shown with this value of the factorisation scale.

On Fig. 4, one can see the LO (in blue) and NLO (in red) μ_R dependence of $\sigma_{\gamma p}$ for J/ψ photoproduction, still using CT18NLO and integrated over P_T and over $z < 0.9$,

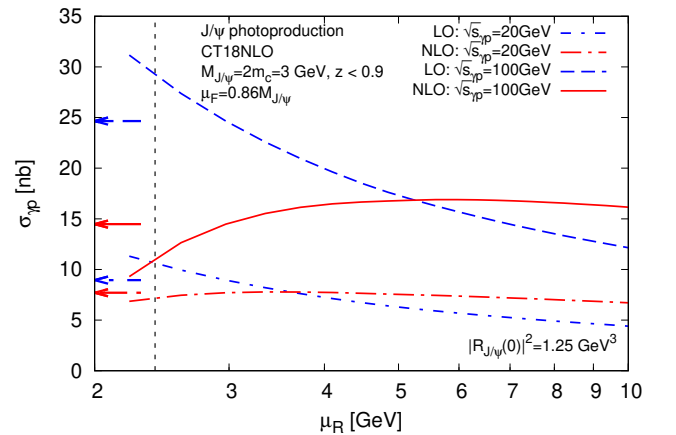


Figure 4: μ_R dependence of $\sigma_{\gamma p}$ at LO and NLO for 2 values of $\sqrt{s_{\gamma p}}$, where the arrows point at the values of $\sigma_{\gamma p}$ for $\mu_R = 3$ GeV. The vertical dashed line delimitates the μ_R region which we use to compute the cross section (see text).

at two values of $\sqrt{s_{\gamma p}} = 20$ GeV (short and long dash-dotted lines) and $\sqrt{s_{\gamma p}} = 100$ GeV (solid and dashed lines). In both cases, the μ_R sensitivity is drastically reduced at NLO. However, one notes that at the higher energy, for $\mu_R \sim M_{J/\psi}$, $\sigma_{\gamma p}^{\text{NLO}}$ is twice smaller than $\sigma_{\gamma p}^{\text{LO}}$ (see the arrows by the y axis). This is due to a large negative contribution from the loops (see the negative dip in the $c_{\gamma g}^{(1)}$ in Fig. 2). Since the LO and NLO cross section are however similar for $\mu_R \sim 2M_{J/\psi}$, the question of the natural scale of the process naturally arises. In fact, as the Born process is $\gamma g \rightarrow Qg$, it appears reasonable to consider $\sqrt{\hat{s}}$ rather than M_Q . A quick LO computation shows that $\sqrt{\langle \hat{s} \rangle}$ ranges from 4 GeV at low hadronic energies up to even 10 GeV at high hadronic energies. In what follows, we thus consider μ_R within the range [2.5 : 10] GeV for J/ψ and, for $\Upsilon(1S)$, $\mu_R \in [8 : 32]$ GeV.

3. Results

Having discussed our methodology, let us now present and analyse our results for J/ψ and $\Upsilon(1S)$ photoproduction cross sections computed at NLO with the $\hat{\mu}_F$ prescription.

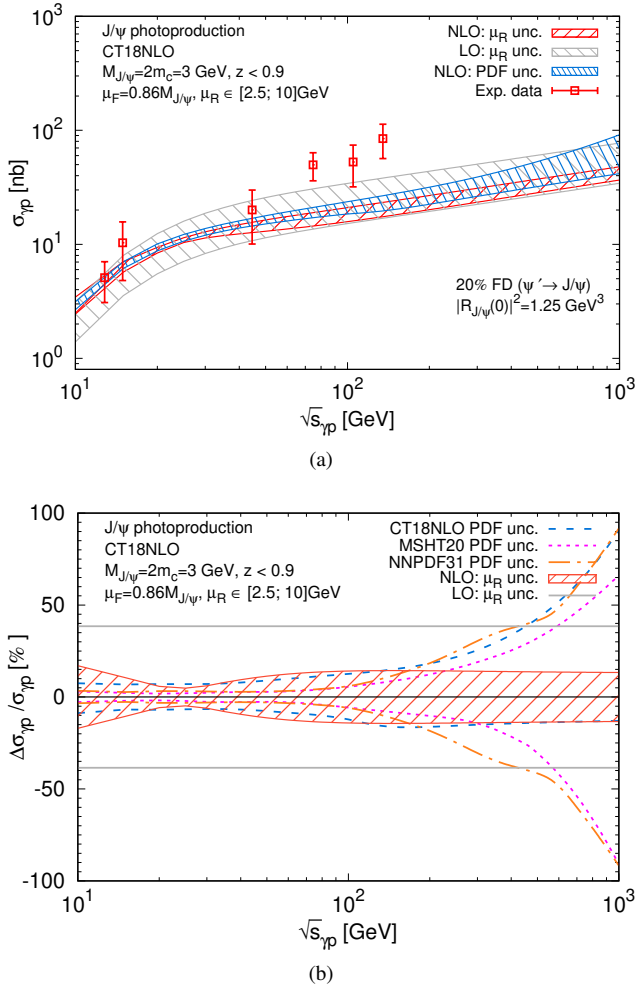


Figure 5: (a) $\sigma_{\gamma p}$ dependence on $\sqrt{s_{\gamma p}}$, (b) $\Delta\sigma_{\gamma p}/\sigma_{\gamma p}$ dependence on $\sqrt{s_{\gamma p}}$ for J/ψ inclusive photoproduction with the μ_R and the PDF uncertainties

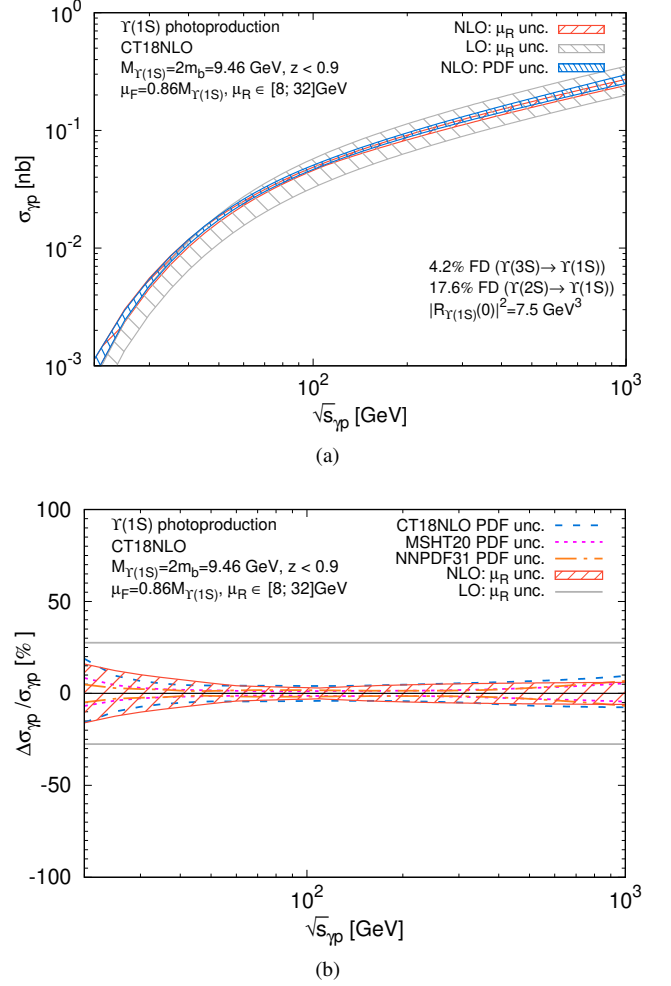


Figure 6: (a) $\sigma_{\gamma p}$ dependence on $\sqrt{s_{\gamma p}}$, (b) $\Delta\sigma_{\gamma p}/\sigma_{\gamma p}$ dependence on $\sqrt{s_{\gamma p}}$ for $\Upsilon(1S)$ inclusive photoproduction with the μ_R and the PDF uncertainties

On Fig. 5 and Fig. 6, we have plotted (a) the cross sections $\sigma_{\gamma p}$ and (b) its (scale and PDF)⁸ relative uncertainty as functions of $\sqrt{s_{\gamma p}}$ for respectively J/ψ and $\Upsilon(1S)$ photoproduction for different PDF sets: CT18NLO [58], MSHT20nlo.as118 [59], NNPDF31_nlo.as.0118.hessian [60]. Let us first discuss Fig. 5a. The LO cross section (grey hatched band) relatively well describes the experimental data points in red. One notes that the NLO μ_R uncertainty (red hatched band) is reduced compared to the LO one, as expected from Fig. 4. The PDF uncertainty at NLO from CT18NLO is shown by the blue hatched band. At large $\sqrt{s_{\gamma p}}$, which corresponds to the low- x region in the proton, it naturally grows and eventually becomes larger than the μ_R uncertainty. Even though it is not an observable physical quantity, we note that with our present set-up (scheme and scale choice) the relative contribution from the γq fusion channel is relatively constant and close to 5% from 20 GeV and above, about 95% then comes from γg fusion.

⁸We note here that the mass and $R(0)$ uncertainties are highly kinematically correlated and essentially translate into a quasi global offset. This is why we focus on both the μ_R and PDF uncertainties.

The increase of the PDF uncertainty is even more visible on the relative uncertainty plots⁹, Fig. 5b, which displays the PDF uncertainties via two curves, dashed blue for CT18NLO, dotted magenta for MSHT20nlo.as118 and dot-dashed orange for NNPDF31_nlo.as_0118_hessian for $\mu_R = 5$ GeV. Above 200 GeV, these are clearly larger than the μ_R one which slightly grows above 50 GeV. This is due to the on-set of the negative contributions from the loop corrections (see below). As for the $\Upsilon(1S)$ case, shown on Fig. 6, the reduction of the μ_R uncertainty at NLO is further pronounced while the PDF and μ_R uncertainties remain similar.

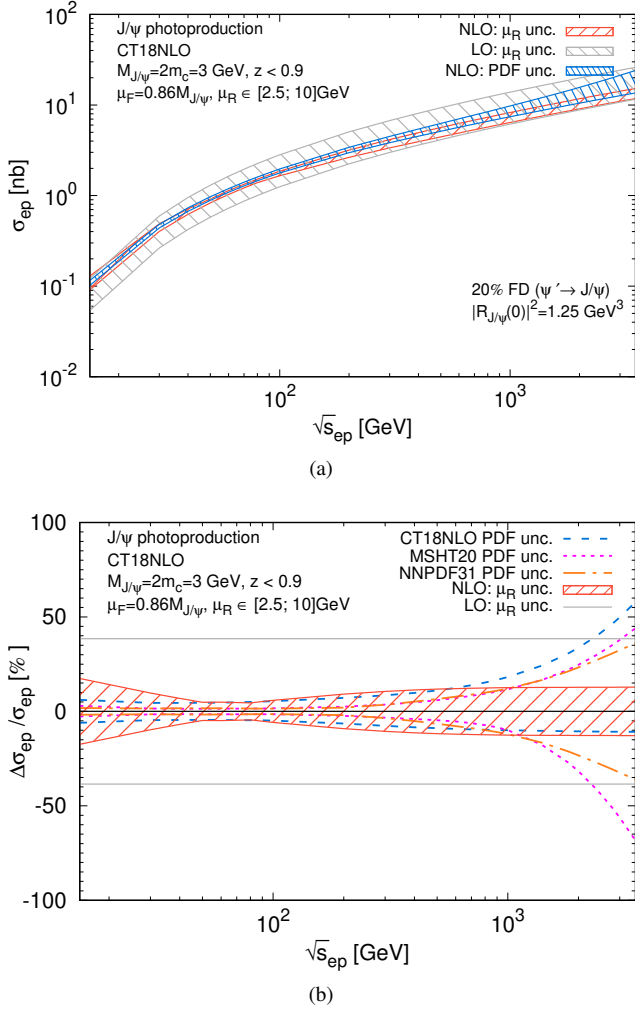


Figure 7: (a) σ_{ep} as a function of $\sqrt{s_{ep}}$, (b) $\Delta\sigma_{ep}/\sigma_{ep}$ as a function of $\sqrt{s_{ep}}$ for J/ψ inclusive photoproduction with its μ_R and PDF uncertainties.

In the J/ψ case, it is clear that it will be important to have at our disposal computations at NNLO accuracy. As Krämer noted [25] long ago, the “virtual+soft” contributions, encapsulated in $c^{(1)}$, are significantly more negative than for open heavy-flavour production [62]. He suggested

⁹For the μ_R relative uncertainty, we computed it as $\pm(\sigma_{\gamma p}^{\max} - \sigma_{\gamma p}^{\min})/(\sigma_{\gamma p}^{\max} + \sigma_{\gamma p}^{\min})$, where $\sigma_{\gamma p}^{\max/\min}$ is the maximum/minimum values of $\sigma_{\gamma p}$ obtained by varying μ_R in the quoted range. For the PDF uncertainties, we used the normalised upper and lower PDF uncertainties [61] for $\mu_R = 5$ GeV for J/ψ and $\mu_R = 16$ GeV for $\Upsilon(1S)$.

that this destructive interference with the Born order amplitude could be due to the momentum transfer of the exchanged virtual gluon, more likely to scatter the $Q\bar{Q}$ pair outside the static limit ($\mathbf{p} \simeq 0$). At NNLO, these one-loop amplitudes will be squared, the two-loop amplitudes will interfere with the Born amplitudes and the amplitudes of the one-loop corrections to the real-emission graphs will also interfere with the real-emission amplitudes. Unless the latter two are subject to the same strong destructive interference effect, one might expect relatively large positive NNLO corrections bringing the cross section close to the upper limit of the LO range and then in better agreement with existing, yet old, data.

At NNLO, we also expect a further reduction of the μ_R uncertainties. This is particularly relevant especially around 50 – 100 GeV, which corresponds to the EIC region. This would likely allow us to better probe gluon PDFs using photoproduction data. Going further, differential measurements in the elasticity or the rapidity could provide a complementary lever arm in x to fit the gluon PDF, even in the presence of sub-leading v colour-octet contributions. Indeed, these would likely exhibit a very similar dependence on x . As we will see later, the expected yields at future facilities, in particular for charmonia, are clearly large enough to perform such differential measurements.

Let us now look at electron-proton cross sections as functions of $\sqrt{s_{ep}}$ for J/ψ (Fig. 7) and $\Upsilon(1S)$ photoproduction (Fig. 8). To obtain them, Eq. (7) was convoluted with the corresponding proton PDFs and a photon flux from the electron. We have used the same photon flux as in [7], where the Weizsäcker-Williams approximation was used:

$$f_{\gamma/e}(x_\gamma, Q_{max}^2) = \frac{\alpha}{2\pi} \times \left[\frac{1 + (1 - x_\gamma)^2}{x_\gamma} \ln \frac{Q_{max}^2}{Q_{min}^2(x_\gamma)} + 2m_e^2 x_\gamma \left(\frac{1}{Q_{max}^2} - \frac{1}{Q_{min}^2(x_\gamma)} \right) \right], \quad (10)$$

where $Q_{min}^2(x_\gamma) = m_e^2 x_\gamma^2 / (1 - x_\gamma)$ and m_e is the electron mass.

On Fig. 7 and Fig. 8, the same colour code and the same parameters than for Fig. 5 and Fig. 6 have been used. For σ_{ep} , one can see the same trends for the μ_R and PDF uncertainties as for $\sigma_{\gamma p}$. It is only at the LHeC energies and above that one could expect to constrain better the PDF uncertainty with such total cross section measurements unless we have at our disposal NNLO computations with yet smaller scale uncertainties.

In Table 1, we provide estimations of the expected number of J/ψ and $\Upsilon(1S)$ possibly detected at the different ep c.m. energies of planned experiments. As it can be seen, the expected yields are always very large for J/ψ which will clearly allow for a number of differential measurements in z , y or $\sqrt{s_{\gamma p}}$. These could then be used to reduce the impact of partially correlated theoretical uncertainties, from the scales and the heavy-quark mass affecting these photoproduction cross sections, in order to bring about some additional constraints on the PDFs at low scales, in particular the gluon one. For $\Upsilon(1S)$, the yields should be sufficient to extract cross sections at the EIC, LHeC and FCC-eh even below

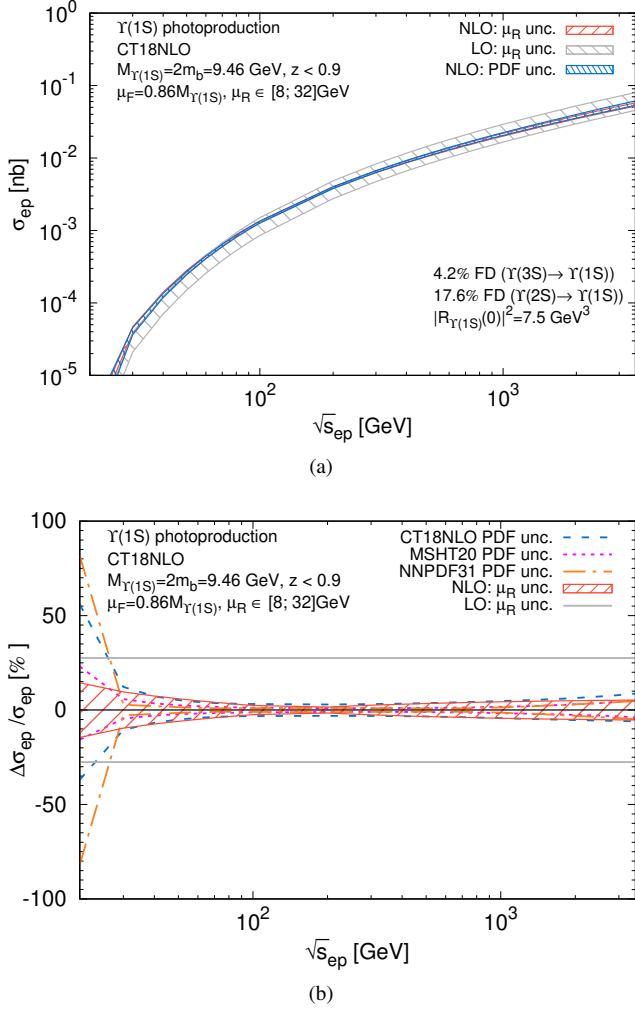


Figure 8: (a) σ_{ep} as a function of $\sqrt{s_{ep}}$, (b) $\Delta\sigma_{ep}/\sigma_{ep}$ as a function of $\sqrt{s_{ep}}$ for $\Upsilon(1S)$ inclusive photoproduction with its μ_R and the PDF uncertainties.

Exp.	$\sqrt{s_{ep}}$	\mathcal{L} (fb $^{-1}$)	$N_{J/\psi}$	$N_{\Upsilon(1S)}$
EicC	16.7	100	$1.5^{+0.3}_{-0.2} \cdot 10^6$	$2.9^{+1.4}_{-1.8} \cdot 10^0$
AMBER	17.3	1	$1.6^{+0.3}_{-0.3} \cdot 10^4$	< 1
EIC	45	100	$8.5^{+0.5}_{-1.0} \cdot 10^6$	$7.8^{+0.9}_{-1.1} \cdot 10^2$
EIC	140	100	$2.5^{+0.1}_{-0.4} \cdot 10^7$	$9.7^{+0.3}_{-0.9} \cdot 10^3$
LheC	1183	100	$9.3^{+2.9}_{-2.9} \cdot 10^7$	$1.0^{+0.05}_{-0.1} \cdot 10^5$
FCC-eh	3464	100	$1.6^{+0.2}_{-1.0} \cdot 10^8$	$2.3^{+0.1}_{-0.3} \cdot 10^5$

Table 1: Expected number of detected quarkonia at NLO at different $\sqrt{s_{ep}}$ (in GeV) corresponding to future facilities (using CT18NLO, $\mu_R = 5$ GeV for J/ψ and $\mu_R = 16$ GeV for $\Upsilon(1S)$, $\mu_F = \hat{\mu}_F$) for $\epsilon_{detect} = 85\%$ via the decay channels to $\mu^+\mu^-$ and e^+e^- , namely $\epsilon_{\ell^+\ell^-}^{J/\psi} \approx 0.1$, and $\epsilon_{\ell^+\ell^-}^{\Upsilon(1S)} \approx 0.04$.

their nominal luminosities.

One can also estimate the expected number of detected ψ' , $\Upsilon(2S)$, $\Upsilon(3S)$ using the following relations

$$\begin{aligned}
 N_{\psi'} &= 0.08 \times N_{J/\psi}, \\
 N_{\Upsilon(2S)} &= 0.52 \times N_{\Upsilon(1S)}, \\
 N_{\Upsilon(3S)} &= 0.4 \times N_{\Upsilon(1S)},
 \end{aligned}
 \tag{11}$$

derived from the values of¹⁰ $|R_Q(0)|^2$ and of the branching fractions to leptons. Using the values in Table 1 and Eq. (11), one can see that the yield of ψ' should be measurable everywhere and the yields of $\Upsilon(2S)$ and $\Upsilon(3S)$ close to about half of that of $\Upsilon(1S)$ should be measurable at the EIC, LHeC and FCC-eh. The proximity between the $\Upsilon(nS)$ yields follows from their similar $|R_Q(0)|^2$ and leptonic branchings.

4. Conclusions

In this work, we have revisited the inclusive photoproduction up to NLO for J/ψ and $\Upsilon(1S)$ at lepton-proton colliders. To this end, we have computed the P_T - and z -integrated σ_{ep} and $\sigma_{\gamma p}$.

Like for other charmonium production processes [27, 63, 64], we have observed the appearance at NLO of negative total cross section which we attribute to an oversubtraction of collinear divergences into the PDF via AP-CT in the $\overline{\text{MS}}$ scheme. We applied the $\hat{\mu}_F$ prescription proposed in [27], which up to NLO corresponds to a resummation of such collinear divergences in High-Energy Factorisation (HEF) [65]. Expressing this integrated cross section in terms of scaling functions exhibiting its explicit μ_R and μ_F scale dependencies, we have found that, for $z < 0.9$, the optimal factorisation scale is $\hat{\mu}_F = 0.86M_Q$ which falls well within the usual ranges of used values. Like for η_c hadroproduction, such a factorisation scale prescription indeed allows one to avoid negative NLO cross sections, but it of course in turn prevents one from studying the corresponding factorisation-scale uncertainties.

We have seen that the NLO μ_R uncertainties get reduced compared to the LO ones but slightly increase around 50 GeV, because of rather large (negative¹¹) interferences between the one-loop and Born amplitudes. As aforementioned, these "virtual+soft" contributions are significantly more negative than for open heavy-flavour production. While Krämer suggested that the difference could stem from the static limit ($\mathbf{p} \approx 0$) specific to the non-relativistic quarkonia, from which one easily departs when gluon exchanges occur, it will certainly be very instructive to have NNLO computations to see whether such one-loop amplitudes squared would bring the cross section back up close to the LO one or whether the interference between the two-loop and the Born amplitudes and between the real-virtual and the real amplitudes would be also negative and large. In any case, it is reasonable to expect a further reduction of the μ_R uncertainties compared to the NLO results.

Then, we have qualitatively investigated the possibility to constrain PDFs using future J/ψ and $\Upsilon(1S)$ photoproduction data. We have seen, unsurprisingly, that PDF uncertainties get larger than the (NLO) μ_R uncertainties with

¹⁰These relations were estimated using $|R_{\psi'}(0)|^2 = 0.8 \text{ GeV}^3$, $|R_{\Upsilon(2S)}(0)|^2 = 5.0 \text{ GeV}^3$ and $|R_{\Upsilon(3S)}(0)|^2 = 3.4 \text{ GeV}^3$.

¹¹Let us stress that unless μ_R is taken very small with a large $\alpha_s(\mu_R)$, these negative contributions are not problematic, unlike the oversubtraction by the AP-CT.

the growth of the γp c.m. energy, in practice from around 300 GeV, *i.e.* for x below 0.01. Although this is above the reach of the future EIC, we hope that with NNLO predictions at our disposal in the future, with yet smaller μ_R uncertainties, one could set novel constraints on PDFs with such EIC measurements. Given our estimated counting rates for 100 fb⁻¹ of ep collisions, we expect that a number of differential measurements will be possible to reduce the impact of highly or even partially correlated theoretical uncertainties, including the contamination of higher- ν corrections such as the colour-octet contributions.

Strictly speaking our predictions for J/ψ and ψ' only regard the prompt yields. An evaluation at NLO of the beauty production cross section points at a feed-down fraction at the 5% level. Given the larger size of the other uncertainties and the possibility to remove it experimentally, we have neglected it. In general though, it will be useful to have a dedicated experimental measurements at the EIC at least to measure the beauty feed down. It may become more significant at low z where the resolved-photon contribution could set in at high $\sqrt{s_{ep}}$, like we have seen [7] it to become the dominant source of J/ψ at large P_T .

Acknowledgements. We thank M. Nefedov and H. Sazdjian for useful discussions and L. Manna for a NLO estimate of the b photoproduction cross section. This project has received funding from the European Union’s Horizon 2020 research and innovation programme under grant agreement No. 824093 in order to contribute to the EU Virtual Access NLOAccess. This project has also received funding from the Agence Nationale de la Recherche (ANR) via the grant ANR-20-CE31-0015 (“PrecisOnium”) and via the IDEX Paris-Saclay ”Investissements d’Avenir” (ANR-11-IDEX-0003-01) through the GLUODYNAMICS project funded by the ”P2IO LabEx (ANR-10-LABX-0038)” and through the Joint PhD Programme of Université Paris-Saclay (ADI). This work was also partly supported by the French CNRS via the IN2P3 project GLUE@NLO, via the Franco-Chinese LIA FCPPL (Quarkonium4AFTER) and via the Franco-Polish EIA (GlueGraph). M.A.O.’s work was partly supported by the ERC grant 637019 “MathAm”. C.F. has been also partially supported by Fondazione di Sardegna under the project “Proton tomography at the LHC”, project number F72F20000220007 (University of Cagliari), and is thankful to the Physics Department of Cagliari University for the hospitality and support for his visit, during which part of the project was done.

Appendix A. Leptonic width and $R(0)$

Up to NNLO, one has [45, 46] (for $\mu_{NRQCD} = m_Q$):

$$\Gamma_{\ell\ell} = \frac{4\pi\alpha^2 e_Q^2 f_Q^2}{3M_Q^2}, f_Q = \sqrt{\frac{3}{\pi M_Q}} |R(0)|^2 \times \left(1 - \frac{8}{3} \frac{\alpha_s(\mu_R)}{\pi} - (44.55 - 0.41n_{lf}) \left(\frac{\alpha_s(\mu_R)}{\pi}\right)^2\right), \quad (\text{A.1})$$

where n_{lf} is the number of active light flavours,

α is the electromagnetic coupling constant, α_s is the strong interaction coupling, M_Q is the Q mass, e_Q is the magnitude of the heavy-quark charge (in units of the electron charge). In Table A.2, we have gathered the resulting radial part of the Schrödinger wave function at the origin of the configuration space at LO, NLO and NNLO for J/ψ and $\Upsilon(1S)$, which were computed from Eq. (A.1) with the measured value of $\Gamma_{\ell\ell}$ [66].

α_s	$ R_{J/\psi}(0) _{\text{LO}}^2$	$ R_{J/\psi}(0) _{\text{NLO}}^2$	$ R_{J/\psi}(0) _{\text{NNLO}}^2$
[0.18,0.34]	0.56	[0.80,1.33]	[1.12,13.5]
α_s	$ R_{\Upsilon}(0) _{\text{LO}}^2$	$ R_{\Upsilon}(0) _{\text{NLO}}^2$	$ R_{\Upsilon}(0) _{\text{NNLO}}^2$
[0.16,0.2]	5.1	[7.0,7.7]	[9.0,11.9]

Table A.2: Values of $R(0)^2$ in GeV³ extracted from the corresponding leptonic widths [66] at LO, NLO and NNLO.

References

- [1] M. Kraemer, “Quarkonium production at high-energy colliders,” *Prog. Part. Nucl. Phys.* **47** (2001) 141–201, [arXiv:hep-ph/0106120 \[hep-ph\]](#).
- [2] **Quarkonium Working Group** Collaboration, N. Brambilla *et al.*, “Heavy quarkonium physics,” [arXiv:hep-ph/0412158 \[hep-ph\]](#).
- [3] J. P. Lansberg, “ J/ψ , ψ' and Υ production at hadron colliders: A Review,” *Int. J. Mod. Phys.* **A21** (2006) 3857–3916, [arXiv:hep-ph/0602091 \[hep-ph\]](#).
- [4] N. Brambilla *et al.*, “Heavy Quarkonium: Progress, Puzzles, and Opportunities,” *Eur. Phys. J.* **C71** (2011) 1534, [arXiv:1010.5827 \[hep-ph\]](#).
- [5] A. Andronic *et al.*, “Heavy-flavour and quarkonium production in the LHC era: from proton–proton to heavy-ion collisions,” *Eur. Phys. J.* **C76** no. 3, (2016) 107, [arXiv:1506.03981 \[nucl-ex\]](#).
- [6] J.-P. Lansberg, “New Observables in Inclusive Production of Quarkonia,” *Phys.Rept.* (2020), [arXiv:1903.09185 \[hep-ph\]](#). (In press).
- [7] C. Flore, J.-P. Lansberg, H.-S. Shao, and Y. Yedelkina, “Large- P_T inclusive photoproduction of J/ψ in electron-proton collisions at HERA and the EIC,” *Phys. Lett. B* **811** (2020) 135926, [arXiv:2009.08264 \[hep-ph\]](#).
- [8] C.-H. Chang, “Hadronic Production of J/ψ Associated With a Gluon,” *Nucl. Phys.* **B172** (1980) 425–434.
- [9] E. L. Berger and D. L. Jones, “Inelastic Photoproduction of J/ψ and Upsilon by Gluons,” *Phys. Rev.* **D23** (1981) 1521–1530.
- [10] R. Baier and R. Ruckl, “Hadronic Collisions: A Quarkonium Factory,” *Z. Phys.* **C19** (1983) 251.
- [11] G. T. Bodwin, E. Braaten, and G. P. Lepage, “Rigorous QCD analysis of inclusive annihilation and production of heavy quarkonium,” *Phys. Rev.* **D51** (1995) 1125–1171, [arXiv:hep-ph/9407339 \[hep-ph\]](#). [Erratum: *Phys. Rev.* **D55**,5853(1997)].
- [12] **H1** Collaboration, S. Aid *et al.*, “Elastic and inelastic photoproduction of J/ψ mesons at HERA,” *Nucl. Phys. B* **472** (1996) 3–31, [arXiv:hep-ex/9603005](#).
- [13] **ZEUS** Collaboration, J. Breitweg *et al.*, “Measurement of inelastic J/ψ photoproduction at HERA,” *Z. Phys. C* **76** (1997) 599–612, [arXiv:hep-ex/9708010](#).
- [14] **ZEUS** Collaboration, S. Chekanov *et al.*, “Measurements of inelastic J/ψ and ψ' photoproduction at HERA,” *Eur. Phys. J. C* **27** (2003) 173–188, [arXiv:hep-ex/0211011](#).
- [15] **H1** Collaboration, C. Adloff *et al.*, “Inelastic photoproduction of J/ψ mesons at HERA,” *Eur. Phys. J. C* **25** (2002) 25–39, [arXiv:hep-ex/0205064 \[hep-ex\]](#).
- [16] **ZEUS** Collaboration, S. Chekanov *et al.*, “Measurement of J/ψ helicity distributions in inelastic photoproduction at HERA,” *JHEP* **12** (2009) 007, [arXiv:0906.1424 \[hep-ex\]](#).

- [17] **H1** Collaboration, F. Aaron *et al.*, “Inelastic Production of J/ψ Mesons in Photoproduction and Deep Inelastic Scattering at HERA,” *Eur. Phys. J. C* **68** (2010) 401–420, [arXiv:1002.0234 \[hep-ex\]](#).
- [18] **ZEUS** Collaboration, H. Abramowicz *et al.*, “Measurement of inelastic J/ψ and ψ' photoproduction at HERA,” *JHEP* **02** (2013) 071, [arXiv:1211.6946 \[hep-ex\]](#).
- [19] H. Jung, G. A. Schuler, and J. Terron, “ J/ψ production mechanisms and determination of the gluon density at HERA,” *Int. J. Mod. Phys. A* **7** (1992) 7955–7988.
- [20] A. Bacchetta, D. Boer, C. Pisano, and P. Tael, “Gluon TMDs and NRQCD matrix elements in J/ψ production at an EIC,” *Eur. Phys. J. C* **80** no. 1, (2020) 72, [arXiv:1809.02056 \[hep-ph\]](#).
- [21] U. D’Alesio, F. Murgia, C. Pisano, and P. Tael, “Azimuthal asymmetries in semi-inclusive J/ψ + jet production at an EIC,” *Phys. Rev. D* **100** no. 9, (2019) 094016, [arXiv:1908.00446 \[hep-ph\]](#).
- [22] R. Kishore, A. Mukherjee, and S. Rajesh, “Sivers asymmetry in the photoproduction of a J/ψ and a jet at the EIC,” *Phys. Rev. D* **101** no. 5, (2020) 054003, [arXiv:1908.03698 \[hep-ph\]](#).
- [23] D. Boer, U. D’Alesio, F. Murgia, C. Pisano, and P. Tael, “ J/ψ meson production in SIDIS: matching high and low transverse momentum,” *JHEP* **09** (2020) 040, [arXiv:2004.06740 \[hep-ph\]](#).
- [24] M. Kramer, J. Zunft, J. Steegborn, and P. M. Zerwas, “Inelastic J/ψ photoproduction,” *Phys. Lett. B* **348** (1995) 657–664, [arXiv:hep-ph/9411372](#).
- [25] M. Kraemer, “QCD corrections to inelastic J/ψ photoproduction,” *Nucl. Phys. B* **459** (1996) 3–50, [arXiv:hep-ph/9508409 \[hep-ph\]](#).
- [26] **H1** Collaboration, S. Aid *et al.*, “Elastic and inelastic photoproduction of J/ψ mesons at HERA,” *Nucl. Phys. B* **472** (1996) 3–31, [arXiv:hep-ex/9603005](#).
- [27] J.-P. Lansberg and M. A. Ozelcik, “Curing the unphysical behaviour of NLO quarkonium production at the LHC and its relevance to constrain the gluon PDF at low scales,” [arXiv:2012.00702 \[hep-ph\]](#).
- [28] A. Accardi *et al.*, “Electron Ion Collider: The Next QCD Frontier: Understanding the glue that binds us all,” *Eur. Phys. J. A* **52** no. 9, (2016) 268, [arXiv:1212.1701 \[nucl-ex\]](#).
- [29] **LHeC Study Group** Collaboration, J. L. Abelleira Fernandez *et al.*, “A Large Hadron Electron Collider at CERN: Report on the Physics and Design Concepts for Machine and Detector,” *J. Phys. G* **39** (2012) 075001, [arXiv:1206.2913 \[physics.acc-ph\]](#).
- [30] **FCC** Collaboration, A. Abada *et al.*, “FCC Physics Opportunities: Future Circular Collider Conceptual Design Report Volume 1,” *Eur. Phys. J. C* **79** no. 6, (2019) 474.
- [31] B. Adams *et al.*, “Letter of Intent: A New QCD facility at the M2 beam line of the CERN SPS (COMPASS+/AMBER),” [arXiv:1808.00848 \[hep-ex\]](#).
- [32] D. P. Anderle *et al.*, “Electron-ion collider in China,” *Front. Phys. (Beijing)* **16** no. 6, (2021) 64701, [arXiv:2102.09222 \[nucl-ex\]](#).
- [33] P. Artoisenet, J. M. Campbell, J. Lansberg, F. Maltoni, and F. Tramontano, “ Υ Production at Fermilab Tevatron and LHC Energies,” *Phys. Rev. Lett.* **101** (2008) 152001, [arXiv:0806.3282 \[hep-ph\]](#).
- [34] J. Lansberg, “On the mechanisms of heavy-quarkonium hadroproduction,” *Eur. Phys. J. C* **61** (2009) 693–703, [arXiv:0811.4005 \[hep-ph\]](#).
- [35] J. Lansberg, “Real next-to-next-to-leading-order QCD corrections to J/ψ and Upsilon hadroproduction in association with a photon,” *Phys. Lett. B* **679** (2009) 340–346, [arXiv:0901.4777 \[hep-ph\]](#).
- [36] B. Gong, J.-P. Lansberg, C. Lorce, and J. Wang, “Next-to-leading-order QCD corrections to the yields and polarisations of J/ψ and Upsilon directly produced in association with a Z boson at the LHC,” *JHEP* **03** (2013) 115, [arXiv:1210.2430 \[hep-ph\]](#).
- [37] J.-P. Lansberg and H.-S. Shao, “Production of $J/\psi + \eta_c$ versus $J/\psi + J/\psi$ at the LHC: Importance of Real α_s^5 Corrections,” *Phys. Rev. Lett.* **111** (2013) 122001, [arXiv:1308.0474 \[hep-ph\]](#).
- [38] J.-P. Lansberg and H.-S. Shao, “ J/ψ -pair production at large momenta: Indications for double parton scatterings and large α_s^5 contributions,” *Phys. Lett. B* **751** (2015) 479–486, [arXiv:1410.8822 \[hep-ph\]](#).
- [39] H.-S. Shao, “Boosting perturbative QCD stability in quarkonium production,” *JHEP* **01** (2019) 112, [arXiv:1809.02369 \[hep-ph\]](#).
- [40] H. Fritzsche, “Producing Heavy Quark Flavors in Hadronic Collisions: A Test of Quantum Chromodynamics,” *Phys. Lett. B* **67** (1977) 217–221.
- [41] F. Halzen, “Cvc for Gluons and Hadroproduction of Quark Flavors,” *Phys. Lett. B* **69** (1977) 105–108.
- [42] H.-S. Shao, “HELAC-Onia: An automatic matrix element generator for heavy quarkonium physics,” *Comput. Phys. Commun.* **184** (2013) 2562–2570, [arXiv:1212.5293 \[hep-ph\]](#).
- [43] H.-S. Shao, “HELAC-Onia 2.0: an upgraded matrix-element and event generator for heavy quarkonium physics,” *Comput. Phys. Commun.* **198** (2016) 238–259, [arXiv:1507.03435 \[hep-ph\]](#).
- [44] R. Barbieri, R. Gatto, R. Kogerler, and Z. Kunszt, “Meson hyperfine splittings and leptonic decays,” *Phys. Lett. B* **57** (1975) 455–459.
- [45] A. Czarnecki and K. Melnikov, “Two loop QCD corrections to the heavy quark pair production cross-section in e^+e^- annihilation near the threshold,” *Phys. Rev. Lett.* **80** (1998) 2531–2534, [arXiv:hep-ph/9712222](#).
- [46] M. Beneke, A. Signer, and V. A. Smirnov, “Two loop correction to the leptonic decay of quarkonium,” *Phys. Rev. Lett.* **80** (1998) 2535–2538, [arXiv:hep-ph/9712302](#).
- [47] P. Marquard, J. H. Piclum, D. Seidel, and M. Steinhauser, “Three-loop matching of the vector current,” *Phys. Rev. D* **89** no. 3, (2014) 034027, [arXiv:1401.3004 \[hep-ph\]](#).
- [48] **CTEQ** Collaboration, R. Brock *et al.*, “Handbook of perturbative QCD: Version 1.0,” *Rev. Mod. Phys.* **67** (1995) 157–248.
- [49] B. Gong and J.-X. Wang, “Next-to-leading-order QCD corrections to e^+e^- to $J/\psi(cc)$ at the B factories,” *Phys. Rev. D* **80** (2009) 054015, [arXiv:0904.1103 \[hep-ph\]](#).
- [50] J. Campbell, J. Huston, and F. Krauss, *The Black Book of Quantum Chromodynamics: A Primer for the LHC Era*. Oxford University Press, 12, 2017.
- [51] T. Kinoshita, “Mass singularities of Feynman amplitudes,” *J. Math. Phys.* **3** (1962) 650–677.
- [52] T. D. Lee and M. Nauenberg, “Degenerate Systems and Mass Singularities,” *Phys. Rev.* **133** (1964) B1549–B1562.
- [53] J.-X. Wang, “Progress in FDC project,” *Nucl. Instrum. Meth. A* **534** (2004) 241–245, [arXiv:hep-ph/0407058](#).
- [54] M. Butenschoen and B. A. Kniehl, “Complete next-to-leading-order corrections to J/ψ photoproduction in nonrelativistic quantum chromodynamics,” *Phys. Rev. Lett.* **104** (2010) 072001, [arXiv:0909.2798 \[hep-ph\]](#).
- [55] T.-J. Hou *et al.*, “New CTEQ global analysis of quantum chromodynamics with high-precision data from the LHC,” *Phys. Rev. D* **103** no. 1, (2021) 014013, [arXiv:1912.10053 \[hep-ph\]](#).
- [56] B. H. Denby *et al.*, “Inelastic and Elastic Photoproduction of J/ψ (3097),” *Phys. Rev. Lett.* **52** (1984) 795–798.
- [57] **NA14** Collaboration, R. Barate *et al.*, “Measurement of J/ψ and ψ' Real Photoproduction on ^6Li at a Mean Energy of 90-GeV,” *Z. Phys. C* **33** (1987) 505.
- [58] T.-J. Hou *et al.*, “Progress in the CTEQ-TEA NNLO global QCD analysis,” [arXiv:1908.11394 \[hep-ph\]](#).
- [59] S. Bailey, T. Cridge, L. A. Harland-Lang, A. D. Martin, and R. S. Thorne, “Parton distributions from LHC, HERA, Tevatron and fixed target data: MSHT20 PDFs,” *Eur. Phys. J. C* **81** no. 4, (2021) 341, [arXiv:2012.04684 \[hep-ph\]](#).
- [60] **NNPDF** Collaboration, R. D. Ball *et al.*, “Parton distributions from high-precision collider data,” *Eur. Phys. J. C* **77** no. 10, (2017) 663, [arXiv:1706.00428 \[hep-ph\]](#).
- [61] A. Buckley, J. Ferrando, S. Lloyd, K. Nordström, B. Page, M. Rüfenacht, M. Schönherr, and G. Watt, “LHAPDF6: parton density access in the LHC precision era,” *Eur. Phys. J. C* **75** (2015) 132, [arXiv:1412.7420 \[hep-ph\]](#).
- [62] J. Smith and W. L. van Neerven, “QCD corrections to heavy flavor photoproduction and electroproduction,” *Nucl. Phys. B* **374** (1992) 36–82.
- [63] M. L. Mangano and A. Petrelli, “NLO quarkonium production in hadronic collisions,” *Int. J. Mod. Phys. A* **12** (1997) 3887–3897, [arXiv:hep-ph/9610364](#).

- [64] Y. Feng, J.-P. Lansberg, and J.-X. Wang, “Energy dependence of direct-quarkonium production in pp collisions from fixed-target to LHC energies: complete one-loop analysis,” *Eur. Phys. J. C* **75** no. 7, (2015) 313, [arXiv:1504.00317 \[hep-ph\]](#).
- [65] J.-P. Lansberg, M. Nefedov, and M. A. Ozcelik, “Matching next-to-leading-order and high-energy-resummed calculations of heavy-quarkonium-hadroproduction cross sections.”. Unpublished.
- [66] **Particle Data Group** Collaboration, P. A. Zyla *et al.*, “Review of Particle Physics,” *PTEP* **2020** no. 8, (2020) 083C01.